RSC Advances

PAPER

View Article Online
View Journal | View Issue

Open Access Article. Published on 04 February 2021. Downloaded on 12/4/2025 3:18:11 PM.
This article is licensed under a Creative Commons Attribution-NonCommercial 3.0 Unported Licence.

Check for updates

Cite this: *RSC Adv.*, 2021, **11**, 6284

Magnetic field effect on the photocatalytic degradation of methyl orange by commercial TiO_2 powder†

Yuecheng Bian,[ab] Ganhong Zheng,[c] Wei Ding,[d] Lin Hu *[ae] and Zhigao Sheng *[ae]

Received 30th September 2020
Accepted 19th January 2021

DOI: 10.1039/d0ra08359c

rsc.li/rsc-advances

In this work, by taking commercial P25 hydrophilic titanium dioxide (TiO_2) as a photocatalyst, the magnetic field effect (MFE) on the photodegradation rate of methyl orange is studied. It is found that a relatively lower magnetic field $B = 0.28$ T can efficiently enhance the photodegradation efficiency of commercial TiO_2 by 24%. However, the photodegradation efficiency of commercial TiO_2 will be suppressed slightly by 7% under a magnetic field of 0.5 T. Moreover, such MFE on the photocatalyst is dependent on the settling state of the reaction solution. Additional experiments on the degradation of other pollutants (methylene blue) and with other photocatalysts (g-C_3N_4) indicate that the MFE is a ubiquitous phenomenon in the photocatalytic degradation process. These observations suggest that the magnetic field can be taken as an efficient strategy to regulate the catalytic process of commercial catalysts and improve the catalytic efficiency.

Introduction

Light is an inexhaustible source of energy. By taking light as a driving force to control the progress of a chemical reaction, it is effective to regulate the chemical reaction. Among all kinds of light related chemical reactions, photocatalysis reaction is a typical reaction that utilizes light as a source of energy.[1,2] Under light radiation, a photocatalyst can trigger and accelerate some important chemical reaction, such as photocatalytic water splitting to produce hydrogen and oxygen, photocatalytic conversion of carbon dioxide, formaldehyde and other gases, and photocatalytic degradation of toxic substances in industrial wastewater and so on.[2–7] It can be seen that photocatalytic reactions have been widely used in modern industrial production and life, and have great industrial application value. For improving the photocatalytic efficiency, researchers mainly carry out study from two directions. The first one is to develop an advanced catalyst with excellent photocatalytic performance to improve the utilization rate of photons.[8,9] For instance, atom doping or hydrogen treating can significantly broaden the spectral response range of titanium dioxide (TiO_2), which covers the spectral response range from ultraviolet to visible band, greatly improving the utilization efficiency of photons.[10,11] The second one is to change the reaction conditions to improve the photocatalytic efficiency,[12] for example, by applying electric field one can significantly influence the transportation process of photoinduced carrier, improving photocatalytic performance.[13] Among the numerous optical activity semiconductor catalysts, titanium dioxide (TiO_2) is a kind of classical optical activity catalyst. In 1972, Fujishima and Honda found for the first time that TiO_2 can degrade water to prepare hydrogen and oxygen under light radiation, and since then, researchers have been committed to develop more effective photochemical transformation reaction systems.[12] For titanium dioxide (TiO_2), there are mainly three crystal types: anatase (~3.2 eV), rutile (~3.02 eV) and brookite (~2.96 eV), in which anatase TiO_2 possesses good optical activity and is an n-type semiconductor with a direct band gap, widely used in optical research including photocatalysts, disinfection, purification, and optical coating materials.[2,14–19]

Magnetic field, as an important thermodynamic parameter similar to temperature and pressure, plays a significant role in numerous physical and chemical processes. For example, in 2004, Y. Tanimoto *et al.* found that paramagnetic transition metal ions could be induced to migrate by gradient magnetic fields, and the movement distance was related to the magnetic susceptibility of ions; larger magnetic susceptibility will result in farther movement distance within the same time.[20] Similarly, in 2004, Chen *et al.* found that magnetic field can accelerate the diffusion of paramagnetic oxygen gas giving rise to an increase in the oxidation reaction rate of $Fe(OH)_2$.[21] Magnetic field can also affect the synthesis of materials besides influencing the migration of ions; for instance, Ding *et al.* found that magnetic field can induce phase transition of MoS_2 from a semiconductor

[a]Anhui Key Laboratory of Condensed Matter Physics at Extreme Conditions, High Magnetic Field Laboratory, Chinese Academy of Sciences, Hefei 230031, China
[b]University of Science and Technology of China, Hefei 230026, China
[c]School of Physics and Materials Science, Anhui University, Hefei 230039, China
[d]Institutes of Physical Science and Information Technology, Anhui University, Hefei 230601, China
[e]Key Laboratory of Photovoltaic and Energy Conservation Materials, Chinese Academy of Sciences, Hefei, 230031, China

† Electronic supplementary information (ESI) available. See DOI: 10.1039/d0ra08359c

© 2021 The Author(s). Published by the Royal Society of Chemistry

Open Access Article. Published on 04 February 2021. Downloaded on 12/4/2025 3:18:11 PM.
This article is licensed under a Creative Commons Attribution-NonCommercial 3.0 Unported Licence.

phase (2H) to metal phase (1 T), and the phase transformation degree depends on the magnetic field intensity, and the pure metal phase (1 T) MoS_2 phase can be obtained when the magnetic field reaches 9 T.[22] Recently, we found that the magnetic field can accelerate the Kirkendall effect of non-magnetic silicon in liquid,[23] and also found that the magnetic field can significantly accelerate the Ostwald ripening process of Fe_3O_4.[24] Undoubtedly, over the past few decades, a great deal of fascinating findings has been achieved under magnetic field. However, there are few studies about how magnetic field influences photocatalysis, especially the MFE on the commercial photocatalysts. In this work, by taking commercial TiO_2 (P25 TiO_2) as the research subject, the MFE on the photodegradation of methyl orange is carefully investigated. The results show that the photodegradation rate can be accelerated under a magnetic field of 0.28 T. Moreover, an unusual phenomenon is observed that the photocatalytic process can be inhibited when a magnetic field of 0.5 T is employed, which is different from the previous reports.

Experimental section

Materials

Titanium dioxide (TiO_2) (99.8% metal basis, anatase phase, hydrophilic type, Aladdin). Methyl orange (96%, Aladdin) deionized water (AR, 25 l, MW = 18.02, Aladdin). Methylene blue (82%+, Adamas). All chemical reagents are of analytical grade and were used directly without further purification.

Synthesis of g-C_3N_4

5 g melamine is put in the ceramic boat with a cover. Then the ceramic boat is placed in the muffle furnace and calcinating the melamine at 520 °C for 2 h, the heating rate is 10 °C min^{-1}.

Photocatalytic experiment

The photocatalytic activities of commercial titanium dioxide TiO_2 were evaluated in terms of its degradation efficiency of methyl orange (10 mg l^{-1}) in water with and without a magnetic field. Typically, 50 mg TiO_2 (g-C_3N_4) powder was dispersed in a 100 ml methyl orange (*., mk/methylene blue) solution with stirring. When the solution is not settled under dark condition some time, the fresh mixing suspension solution of methyl orange is obtained. To achieve the adsorption–desorption equilibrium of methyl orange on the surface of the catalysts, the mixed solution was kept for 48 h in the dark. Subsequently, the suspension solution is radiated by a 300 W xenon lamp. Because a permanent magnet was employed in the experiment, the conventional magneton agitation could not be used. Therefore, an inert gas (N_2) was used to agitate the reaction solution, and the gas velocity was controlled to be constant at 80 ml min^{-1} with a gas flowmeter. The current value was fixed at 21 A of xenon lamp. Finally, the residual methyl orange concentration in the supernatant was analyzed by UV-visible spectrophotometry (UV-2102 PC) at certain intervals.

Characterizations

The microcosmic morphological and structural information of samples were obtained by field emission scanning electron microscopy (FE-SEM, FEI-designed Sirion 200, Hillsboro, OR) and transmission electron microscopy (TEM, JEM-2010, JEOL Ltd., Japan). The crystalline structure of the samples was identified by a powder X-ray diffractometer using Cu Kα radiations (XRD, X'Pert Pro MPD, $\lambda = 1.54056$ Å). The electron spin resonance (ESR) spectroscopy of the sample was obtained with a Bruker EMX plus 10/12 (equipped with Oxford ESR910 Liquid Helium cryostat) at room temperature.

Results and discussion

Due to the small size of the particles and therefore large surface energy, commercial TiO_2 is present in an agglomerate state, as shown in the SEM image (Fig. 1a). Based on the X-ray diffraction (XRD) data (Fig. 1b), TiO_2 is indexed to the pure anatase phase with an average diameter of ~10.26 nm. In order to further characterize the energy band information of TiO_2, UV-visible absorption spectroscopy was carried out at room temperature, and the result is shown in Fig. 1c. The band gap of TiO_2 was calculated to be about ~3.16 eV using the Tauc formula: $(\alpha h\nu)^n = A(h\nu - E_g)$,[25] which corresponds to a wavelength of ~392 nm, and the absorption band belongs to the ultraviolet band. Fig. 1d gives the photoluminescence (PL) spectrum at room temperature, which is consistent with the UV-visible absorption spectrum.

In the experiment, a suitable experimental equipment was designed, as shown in Fig. 2. Due to the need for applying a magnetic field to the reaction vessel, the conventional magneton agitation could not be used. Therefore, an inert gas (N_2) was used to agitate the reaction solution, and the gas velocity in the experiment was controlled to be constant at 80 ml min^{-1} with a gas flowmeter. The small commercial circular flake magnets were employed to provide a magnetic field environment. The intensity of the magnetic field was changed by changing the number of small magnets. The specific value of the magnetic field strength was measured by a Gauss meter. In each comparison experiment, except for changing the intensity of the magnetic field, other reaction conditions were kept consistent. The distance between the xenon lamp and the reaction vessel was controlled by adjusting the height of the xenon lamp.

The photodegradation process of methyl orange mainly involves two processes: the adsorption equilibrium process between the catalyst and methyl orange, and the other one is the degradation process of methyl orange on the catalyst surface. Therefore, in the experiment, the mixed solution of methyl orange and TiO_2 was first treated under two different conditions including non-settling and settling for 48 h, and then the variation of methyl orange concentration was studied by obtaining the ultraviolet-visible absorption spectrum. As shown in Fig. S1a,† after settling for 48 hours under dark, the characteristic absorption peak intensity of methyl orange decreases evidently compared to the non-settling condition. This result

Open Access Article. Published on 04 February 2021. Downloaded on 12/4/2025 3:18:11 PM.
This article is licensed under a Creative Commons Attribution-NonCommercial 3.0 Unported Licence.

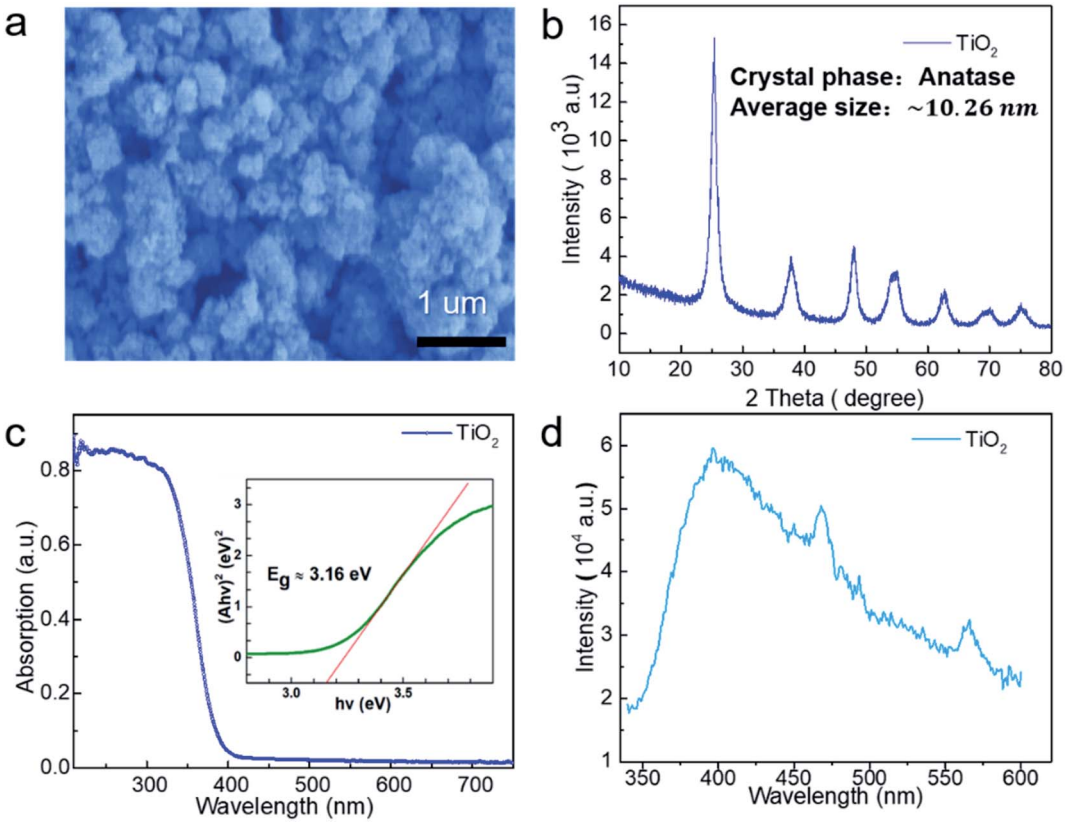

Fig. 1 (a) Scanning Electron Microscopy (SEM) image of TiO_2. (b) X-ray diffraction pattern (XRD) of TiO_2. (c) UV-visible absorption spectrum (inset: Tauc plot, shows the band gap of TiO_2: $E_g = 3.16$ eV). (d) Photoluminescence (PL) spectrum of TiO_2 at room temperature.

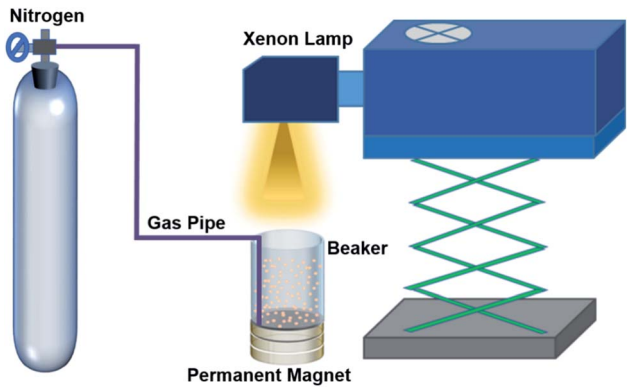

Fig. 2 Schematic diagram of experimental setup.

indicates that there is an obvious adsorption equilibrium process between TiO_2 and methyl orange, which has an important influence on the photocatalytic process. During the photodegradation process of methyl orange dye, transient radical intermediates, such as free radicals ($^{\bullet}OH$, $^{\bullet}O^{2-}$), were generated. Therefore, by using DMPO (5,5-dimethyl-1-pyrroline *N*-oxide) as the trapping agent, the measurement of ESR was carried out at room temperature for the methyl orange solution under ultraviolet light irradiation in the presence of commercial TiO_2. Fig. S1b† shows the ESR signals of DMPO–$^{\bullet}OH$ of the methyl orange solution before and after ultraviolet light illumination. A quartet line profile with a 1 : 2 : 2 : 1 intensity pattern of DMPO–$^{\bullet}OH$ ESR signal can be seen when the measurement was performed under ultraviolet light irradiation, while only a weak ESR signal can be observed for DMPO–$^{\bullet}OH$ without light irradiation. This measurement result is well consistent with the spectra reported in the literature for the DMPO–$^{\bullet}OH$ adduct and confirms the formation of $^{\bullet}OH$ radicals during the irradiation of TiO_2.[26,27] Further, by comparing the color of the two solutions obtained with different light illumination time ($t = 0$ min and $t = 60$ min) (Fig. S1b†), it can also be observed clearly that the color of the reaction solution with ultraviolet radiation is significantly lighter than that without light radiation. This demonstrates that commercial TiO_2 can effectively degrade the methyl orange dye under ultraviolet light irradiation.

In order to study the MFE on the photocatalytic reaction of TiO_2, we conducted photocatalytic experiments under different magnetic field intensities. First, we performed photocatalytic experiments with non-settling mixed solutions. The typical results are shown in Fig. 3. Fig. 3a shows the photocatalytic results under zero field ($B = 0$ T), where it can be seen that the strength of the characteristic absorption peak of methyl orange decreases gradually with reaction time, indicating that methyl orange is decomposed gradually. Fig. 3b shows the experimental result under a magnetic field of $B = 0.28$ T. It can be

 © 2021 The Author(s). Published by the Royal Society of Chemistry

Open Access Article. Published on 04 February 2021. Downloaded on 12/4/2025 3:18:11 PM.
This article is licensed under a Creative Commons Attribution-NonCommercial 3.0 Unported Licence.

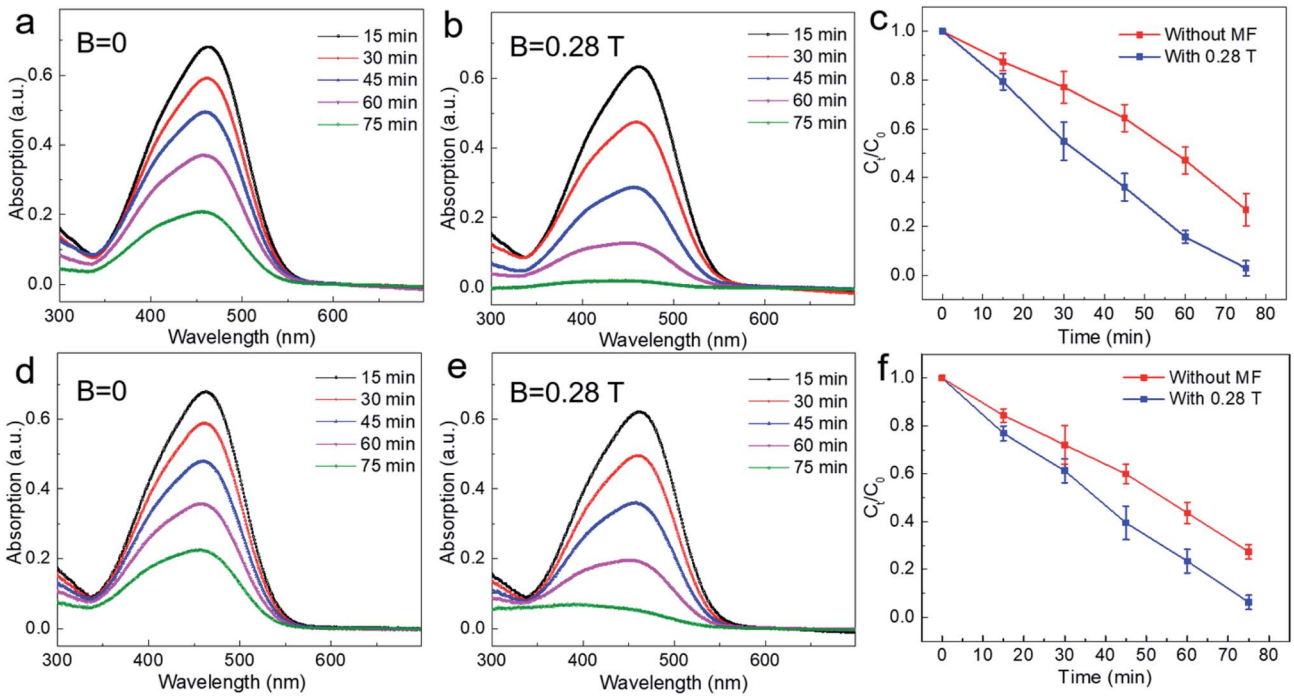

Fig. 3 UV-visible absorption spectra of non-settling and after settling for 48 h methyl orange solution with different degradation time, respectively. For non-settling condition, (a) without magnetic field, and (b) with a low magnetic field $B = 0.28$ T, respectively. (c) Variation of degradation rate with time without and with a magnetic field $B = 0.28$ T. For settling 48 h condition, (d) without magnetic field, and (e) with a low magnetic field $B = 0.28$ T, respectively. (f) Variation of degradation rate with time under without and with a magnetic field $B = 0.28$ T (the error bars of experimental data are obtained from repeating the experiment three times under the same experimental conditions).

found that the strength of the characteristic absorption peak of methyl orange decreases more obviously after a magnetic field is applied. For example, at reaction time $t = 75$ min, there are still obvious characteristic absorption peaks without magnetic fields (Fig. 3a); however, the characteristic absorption peak of methyl orange solution almost disappeared under the magnetic field of 0.28 T (Fig. 3b), which indicates that methyl orange was almost completely degraded when the magnetic field ($B = 0.28$ T) was applied. Then, we extracted the strength of the characteristic absorption peak at different degradation times with or without magnetic field and plotted the variation of degradation rates of methyl orange with time (Fig. 3c). It can be seen that the degradation rate of methyl orange increases after applying a magnetic field of 0.28 T. For example, when $t = 75$ min, the degradation rate increased by ~24% with magnetic field compared with that of zero magnetic field ($B = 0$ T).

Then, in order to further study the magnetic effect on the solution after settling for 48 h under dark, the corresponding photocatalytic measurements with or without magnetic field same as non-settling condition were carried out. As shown in Fig. 3d–f, it can be seen that the degradation rate of methyl orange is largely increased after applying a magnetic field of 0.28 T and increased by about ~21% when the degradation time was at $t = 75$ min, which is almost the same as non-settling experimental results. These results indicate that applying a magnetic field of 0.28 T can give an obvious positive magnetic effect for either non-settling or settling conditions, that is, it accelerates the photocatalytic reaction. The likely explanations can be summarized as follows. For the adsorption process, the movement of charged particles in the solution can be affected effectively by the Lorentz force produced by the magnetic field.[28,29] Moreover, the surface of TiO_2 particles contains a lot of dangling bonds that can be polarized easily under the magnetic field, resulting in the reduction of surface adsorption energy. These two factors are beneficial for the adsorption of dye molecules on the surface of TiO_2.[30] As seen from Fig. 3c and f, the magnetic field effects on the methyl orange degradation rate is more obvious for the non-settling condition before 30 min, and final degradation rates of both conditions including non-settling and settling is the same at $t = 75$ min under magnetic field, which indicates that magnetic fields benefit from the adsorption equilibrium between TiO_2 and methyl orange. On the other hand, for the chemical reaction occurring on the surface of TiO_2, the electron transfer rate determines the speed of the chemical reaction. Previous studies have shown that Lorentz force can affect the movement of charge effectively. For our experiment, when the photons radiate to the surface of TiO_2, the energy of these photons is absorbed by the electrons in the valence band of TiO_2, stimulating the electron transition from the valence band to the conduction band to form photo-induced carriers (electron–hole pair). After a magnetic field is applied, the Lorentz force can effectively separate the electron–hole pair to suppress carrier recombination, improving the utilization efficiency of the photoinduced carrier.[31] Additionally, from the perspective of the diffusion length of the carrier, the diffusion lengths of the hole and electron are about 10 nm and

Open Access Article. Published on 04 February 2021. Downloaded on 12/4/2025 3:18:11 PM.
This article is licensed under a Creative Commons Attribution-NonCommercial 3.0 Unported Licence.

10 mm, respectively. In our work, the average particle diameter of TiO_2 is ~10 nm, therefore, the magnetic effect induced by the Lorentz force upon carrier motion is more obvious.[32]

In order to further study the photocatalytic effect of TiO_2 under a relatively high magnetic field, experiments similar to those under a low magnetic field were also carried out. For the non-settling mixed solution of TiO_2 and methyl orange, photocatalytic experiments were performed both under zero field ($B = 0$ T) and a magnetic field ($B = 0.5$ T). As shown in Fig. 4a and b, the characteristic absorption peak intensity of methyl orange reduced only slightly after applying a magnetic field of 0.5 T. Then, for the mixed solution of TiO_2 and methyl orange allowed to settle for 48 h under dark, the photocatalytic experiment was carried out in the same way. It can be seen that the experimental results are similar to the non-settling experimental results with and without a magnetic field of 0.5 T (Fig. 4d and e). By comparing the experimental result of photocatalysis with that of under zero field, it can be found that the higher magnetic field ($B = 0.5$ T) has an obviously negative magnetic effect on the photodegradation of methyl orange, that is, the magnetic field has an inhibitory effect on the photocatalytic reaction. From the experimental results shown in Fig. 4c and f, it can be seen that the photodegradation efficiency of methyl orange is suppressed obviously by a magnetic field of 0.5 T. For example, when the degradation time was at $t = 75$ min, the degradation rate of methyl orange was reduced by 7% when a magnetic field $B = 0.5$ T was applied. According to previous studies, the magnetic field always has a positive magnetic effect for some reported catalysts, that is, the magnetic field can accelerate the photocatalytic reaction.[31,33–35] Interestingly, our experimental results show that for commercial photocatalyst TiO_2, the magnetic field effect is dependent on the magnetic field intensity during the degradation reaction of methyl orange. When a relatively high magnetic field is employed, the photocatalytic reaction can be suppressed.

As mentioned above, the photocatalytic reaction involves both adsorption and chemical reaction. The experimental results under 0.5 T magnetic field indicate that the magnetic field may inhibit the chemical reaction of the degraded substance on the surface of catalyst. Here, following two dynamic processes should be involved in the surface chemical reaction process: one is the generation and separation of photoinduced carriers subsequently transferred to the surface of the catalyst; the other one is the charge transfer process occurring between the carriers transferred to the surface of the catalyst and the dye molecule (methyl orange molecule). It was observed that the magnetic field has an inhibitory effect on the recombination of photoinduced carriers, that is, the existence of the magnetic field is conducive to the separation of photoinduced carriers, thus facilitating the efficiency of the photocatalytic reaction.[31] Therefore, the suppressed effect of magnetic field on photocatalysis observed in our work might be related to the charge transfer process between photoinduced carriers and dye molecules adsorbed on the surface of the

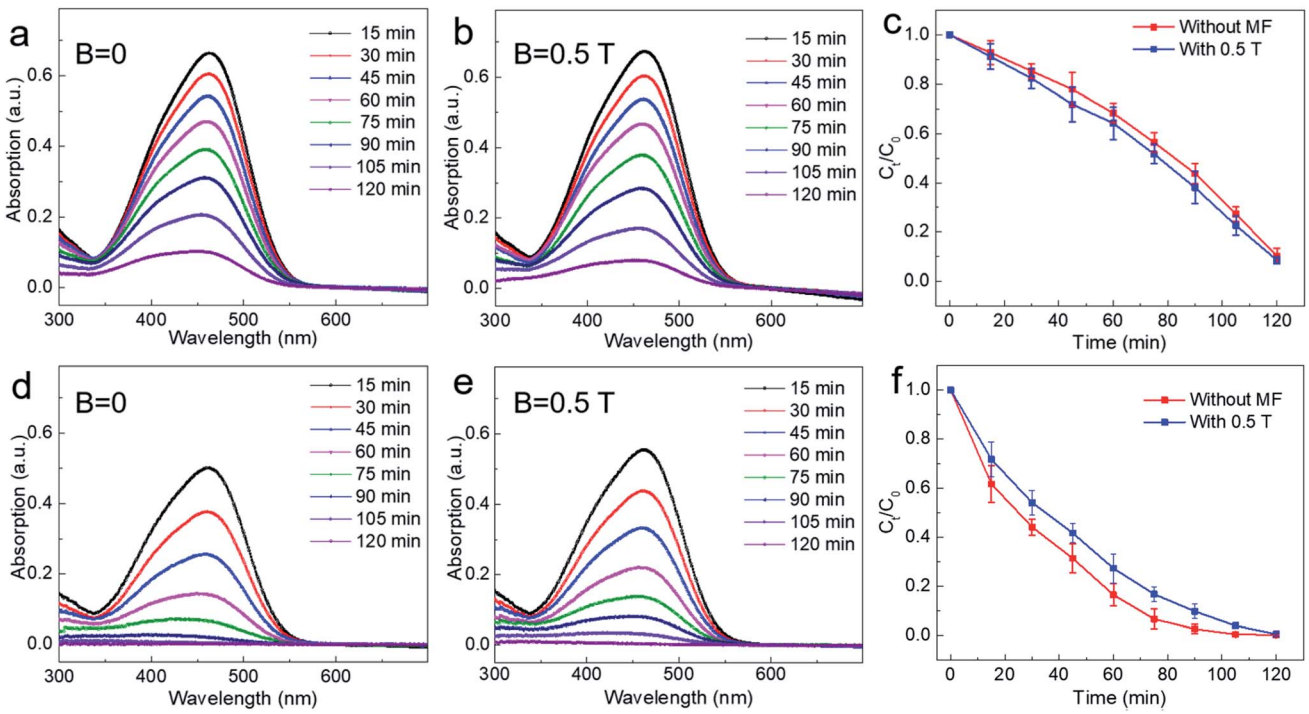

Fig. 4 UV-visible absorption spectra of non-settling and after settling for 48 h methyl orange solution with different degradation time, respectively. For non-settling condition, (a) without magnetic field, and (b) with a high magnetic field $B = 0.5$ T, respectively. (c) Variation of degradation rate with time without and with a magnetic field $B = 0.5$ T. For settling 48 h condition, (d) without magnetic field, and (e) with a high magnetic field $B = 0.5$ T, respectively. (f) Variation of degradation rate with time without and with a magnetic field $B = 0.5$ T (the error bars of experimental data are obtained from repeating the experiment three times under the same experimental conditions).

 © 2021 The Author(s). Published by the Royal Society of Chemistry

Open Access Article. Published on 04 February 2021. Downloaded on 12/4/2025 3:18:11 PM.
This article is licensed under a Creative Commons Attribution-NonCommercial 3.0 Unported Licence.

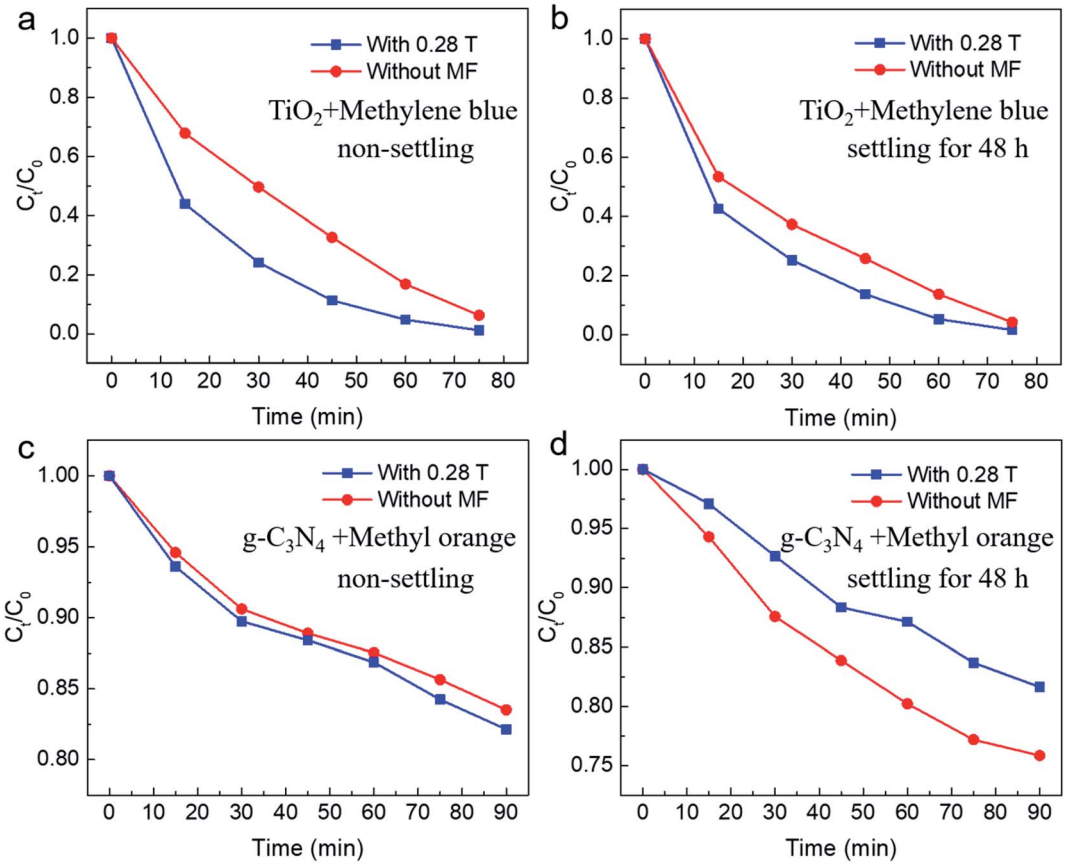

Fig. 5 Variation of the degradation rate of non-settling and settling for 48 h solution with different degradation time under low magnetic field (B = 0.28 T), respectively. By taking TiO_2 as the photocatalyst, (a) and (b) show the photodegradation of methylene blue for non-settling condition and settling for 48 h, respectively. By taking g-C_3N_4 as the photocatalyst, (c) and (d) show the photodegradation of methyl orange for non-settling and settling for 48 h, respectively.

catalyst. Under a relatively higher magnetic field, the Lorentz force exerted by the magnetic field is larger, which will accelerate the motion of the charged particles in reaction system and therefore might produce an adverse effect on the survival of carriers and the subsequent charge transfer process between the catalyst and dye molecules, thus showing a suppressed effect on the photocatalytic reaction. For further studying the magnetic field effect mechanism, the active species trapping experiment was performed under the same condition for non-settling methyl orange solution. In order to ascertain the active species in the degradation process, some sacrificial agents, such as ammonia solution (OA), isopropanol (IPA), and 1,4-benzoquinone (BQ) were used as the hole (h^+) scavenger, hydroxyl radical ($^{\bullet}OH$) scavenger, and superoxide radical ($^{\bullet}O^{2-}$) scavenger, respectively. From the typical result as shown in Fig. S2,† it can be seen that all active species are involved in the photodegradation of methyl orange (MO) when the magnetic field was B = 0.28 T. However, the hydroxyl radical ($^{\bullet}OH$) was affected and made a small contribution to the photodegradation of methyl orange (MO) when a high magnetic field (B = 0.5 T) was applied. However, the more detailed mechanism needs to be further explained by combining further experiments and theories. The influence of magnetic field for the stability of commercial TiO_2 was also explored. As shown in Fig. S3–S5,† there are negligible changes observed in SEM, TEM and XRD characterizations for commercial TiO_2 before and after the photocatalytic reaction. More interestingly, photocatalytic cycle results for non-settling and settling solution show no obvious changes of the MFE on the photocatalytic process, which further confirms the stability of the commercial TiO_2 used under the magnetic field (Fig. S6†). Further, similar phenomena are also observed in other dyes and photocatalysts, including TiO_2 photodegradation of methylene blue, and g-C_3N_4 photodegradation of methyl orange. As shown in Fig. 5a and b, for TiO_2 photodegradation of methylene blue, an obvious magnetic field acceleration effect under the low magnetic field (B = 0.28 T) can be observed, whereas it shows a light magnetic field acceleration effect for the high magnetic field (B = 0.5 T, Fig. S7b†). Further, after settling the methylene blue solution for 48 h, the magnetic field acceleration effect was smaller than that of the non-settling mixed reaction solution (B = 0.28 T, Fig. 5b). Moreover, the suppressed effect on the photodegradation of methylene blue was also observed when a high magnetic field (B = 0.5 T, Fig. S7d†) was applied. At the same time, a magneto-dependent relation can be observed for the photodegradation of methyl orange when g-C_3N_4 was used as

Open Access Article. Published on 04 February 2021. Downloaded on 12/4/2025 3:18:11 PM.
This article is licensed under a Creative Commons Attribution-NonCommercial 3.0 Unported Licence.

the photocatalyst for photodegrading methyl orange (Fig. S8†). For the non-settling methyl orange solution, the magnetic field acceleration effect increases with the increase in the magnetic field (Fig. 5c and S8†), although the acceleration effect is small since pure g-C_3N_4 generally shows a low photodegradation performance compared with TiO_2. However, for the reaction solution after settling for 48 h, the magnetic field shows a suppressed effect for both low and high magnetic fields (Fig. 5d and S8†). As mentioned above, an adsorption process occurs between the photocatalyst and the pollutant. Here, the acceleration effect might be attributed to the magnetic fields, which promote the adsorption equilibrium process.

Conclusion

In summary, the MFE on the photodegradation of methyl orange by a commercial photocatalyst (TiO_2) was studied carefully. With a low magnetic field of 0.28 T, the magnetic field can increase the photodegradation rate efficiently in the presence of TiO_2. However, when a magnetic field of 0.5 T is applied, the photodegradation reaction of methyl orange will be suppressed. It should be emphasized that all these experiments are done with commercial P25 TiO_2 powder. These results provide a novel magneto-method to modulate the photocatalysis process, which may find potential applications in catalysis.

Conflicts of interest

The authors declare no conflict of interest.

Acknowledgements

We gratefully acknowledge financial support from the National Key R&D Program of China (grant no. 2016YFA0401803), the National Natural Science Foundation of China (NSFC; grant no. 11574316, U1532155), the Key Research Program of Frontier Sciences, CAS (grant no. QYZDB-SSW-SLH011), Key Lab of Photovoltaic and Energy Conservation Materials, Chinese Academy of Sciences (grant no. PECL2019QN004). A portion of this work was performed on the Steady High Magnetic Field Facilities, High Magnetic Field Laboratory, CAS. We thank Le Zhou and Kaibin Li from Institute of Solid State Physics, Chinese Academy of Sciences for fruitful discussions and improvement of our manuscript.

References

1 M. R. Hoffmann, S. T. Martin, W. Y. Choi and D. W. Bahnemann, Environmental applications of semiconductor photocatalysis, *Chem. Rev.*, 1995, **95**(1), 69–96.
2 A. L. Linsebigler, G. Q. Lu and J. T. Yates, Photocatalysis on TiO_2 surfaces - principles, mechanisms, and selected results, *Chem. Rev.*, 1995, **95**(3), 735–758.
3 A. Kudo and Y. Miseki, Heterogeneous photocatalyst materials for water splitting, *Chem. Soc. Rev.*, 2009, **38**(1), 253–278.
4 S. N. Habisreutinger, L. Schmidt-Mende and J. K. Stolarczyk, Photocatalytic Reduction of CO_2 on TiO_2 and Other Semiconductors, *Angew. Chem., Int. Ed.*, 2013, **52**(29), 7372–7408.
5 X. Chen, S. Shen, L. Guo and S. S. Mao, Semiconductor-based Photocatalytic Hydrogen Generation, *Chem. Rev.*, 2010, **110**(11), 6503–6570.
6 P. Zhang, T. Wang, X. Chang and J. Gong, Effective Charge Carrier Utilization in Photocatalytic Conversions, *Acc. Chem. Res.*, 2016, **49**(5), 911–921.
7 H. Wang, L. Zhang, Z. Chen, J. Hu, S. Li, Z. Wang, J. Liu and X. Wang, Semiconductor heterojunction photocatalysts: design, construction, and photocatalytic performances, *Chem. Soc. Rev.*, 2014, **43**(15), 5234–5244.
8 W. J. Ong, L. L. Tan, Y. H. Ng, S. T. Yong and S. P. Chai, Graphitic Carbon Nitride (g-C_3N_4)-Based Photocatalysts for Artificial Photosynthesis and Environmental Remediation: Are We a Step Closer To Achieving Sustainability?, *Chem. Rev.*, 2016, **116**(12), 7159–7329.
9 H. Yi, M. Yan, D. L. Huang, G. M. Zeng, C. Lai, M. F. Li, X. Q. Huo, L. Qin, S. Y. Liu, X. G. Liu, B. S. Li, H. Wang, M. C. Shen, Y. K. Fu and X. Y. Guo, Synergistic effect of artificial enzyme and 2D nano-structured Bi_2WO_6 for eco-friendly and efficient biomimetic photocatalysis, *Appl. Catal., B*, 2019, **250**, 52–62.
10 R. Asahi, T. Morikawa, T. Ohwaki, K. Aoki and Y. Taga, Visible-light photocatalysis in nitrogen-doped titanium oxides, *Science*, 2001, **293**(5528), 269–271.
11 X. Chen, L. Liu, P. Y. Yu and S. S. Mao, Increasing Solar Absorption for Photocatalysis with Black Hydrogenated Titanium Dioxide Nanocrystals, *Science*, 2011, **331**(6018), 746–750.
12 A. Fujishima and K. Honda, Electrochemical photolysis of water at a semiconductor electrode, *Nature*, 1972, **238**(5358), 37–38.
13 H. Wu, H. L. Tan, C. Y. Toe, J. Scott, L. Wang, R. Amal and Y. H. Ng, Photocatalytic and Photoelectrochemical Systems: Similarities and Differences, *Adv. Mater.*, 2020, **32**(18), 1904717.
14 A. W. Xu, Y. Gao and H. Q. Liu, The preparation, characterization, and their photocatalytic activities of rare-earth-doped TiO_2 nanoparticles, *J. Catal.*, 2002, **207**(2), 151–157.
15 H. Li, Z. Bian, J. Zhu, D. Zhang, G. Li, Y. Huo, H. Li and Y. Lu, Mesoporous titania spheres with tunable chamber structure and enhanced photocatalytic activity, *J. Am. Chem. Soc.*, 2007, **129**(27), 8406–8407.
16 J. Zhang, Q. Xu, Z. Feng, M. Li and C. Li, Importance of the relationship between surface phases and photocatalytic activity of TiO_2, *Angew. Chem., Int. Ed.*, 2008, **47**(9), 1766–1769.
17 K. Woan, G. Pyrgiotakis and W. Sigmund, Photocatalytic Carbon-Nanotube-TiO_2 Composites, *Adv. Mater.*, 2009, **21**(21), 2233–2239.
18 X. Han, Q. Kuang, M. Jin, Z. Xie and L. Zheng, Synthesis of Titania Nanosheets with a High Percentage of Exposed

 © 2021 The Author(s). Published by the Royal Society of Chemistry

Open Access Article. Published on 04 February 2021. Downloaded on 12/4/2025 3:18:11 PM.
This article is licensed under a Creative Commons Attribution-NonCommercial 3.0 Unported Licence.

(001) Facets and Related Photocatalytic Properties, *J. Am. Chem. Soc.*, 2009, **131**(9), 3152–3153.

19 D. O. Scanlon, C. W. Dunnill, J. Buckeridge, S. A. Shevlin, A. J. Logsdail, S. M. Woodley, C. R. A. Catlow, M. J. Powell, R. G. Palgrave, I. P. Parkin, G. W. Watson, T. W. Keal, P. Sherwood, A. Walsh and A. A. Sokol, Band alignment of rutile and anatase TiO_2, *Nat. Mater.*, 2013, **12**(9), 798–801.

20 M. Fujiwara, K. Chie, J. Sawai, D. Shimizu and Y. Tanimoto, On the movement of paramagnetic ions in an inhomogeneous magnetic field, *J. Phys. Chem. B*, 2004, **108**(11), 3531–3534.

21 Z. M. Peng, J. Wang, Y. J. Huang and Q. W. Chen, Magnetic field-induced increasing of the reaction rates controlled by the diffusion of paramagnetic gases, *Chem. Eng. Technol.*, 2004, **27**(12), 1273–1276.

22 W. Ding, L. Hu, J. Dai, X. Tang, R. Wei, Z. Sheng, C. Liang, D. Shao, W. Song, Q. Liu, M. Chen, X. Zhu, S. Chou, X. Zhu, Q. Chen, Y. Sun and S. X. Dou, Highly Ambient-Stable 1T-MoS_2 and 1T-WS_2 by Hydrothermal Synthesis under High Magnetic Fields, *ACS Nano*, 2019, **13**(2), 1694–1702.

23 Y. C. Bian, W. Ding, L. Hu, Z. W. Ma, L. Cheng, R. R. Zhang, X. B. Zhu, X. W. Tang, J. M. Dai, J. Bai, Y. P. Sun and Z. G. Sheng, Acceleration of Kirkendall effect processes in silicon nanospheres using magnetic fields, *CrystEngComm*, 2018, **20**(6), 710–715.

24 W. Ding, L. Hu, Z. G. Sheng, J. M. Dai, X. B. Zhu, X. W. Tang, Z. Z. Hui and Y. P. Sun, Magneto-acceleration of Ostwald ripening in hollow Fe_3O_4 nanospheres, *CrystEngComm*, 2016, **18**(33), 6134–6137.

25 J. Tauc, R. Grigorovici and A. Vancu, Optical properties and electronic structure of amorphous germanium, *Phys. Status Solidi*, 1966, **15**(2), 627–637.

26 Z. F. Yao, Z. X. Dai, Z. J. Zhang, G. H. Zheng and X. Xu, Visible-light-driven photocatalytic degradation using Mn-doped $SrMoO_4$ nanoparticles, *Appl. Organomet. Chem.*, 2019, **33**(4), 10.

27 Z. Wang, W. Ma, C. Chen, H. Ji and J. Zhao, Probing paramagnetic species in titania-based heterogeneous photocatalysis by electron spin resonance (ESR) spectroscopy-A mini review, *Chem. Eng. J.*, 2011, **170**(2–3), 353–362.

28 T. H. Hsieh and H. J. Keh, Electrokinetic motion of a charged colloidal sphere in a spherical cavity with magnetic fields, *J. Chem. Phys.*, 2011, **134**(4), 7.

29 Y. Kinouchi, S. Tanimoto, T. Ushita, K. Sato, H. Yamaguchi and H. Miyamoto, Effects of static magnetic-fields on diffusion in solutions, *Bioelectromagnetics*, 1988, **9**(2), 159–166.

30 R. Li, Y. Yang, R. Li and Q. Chen, Experimental and Theoretical Studies on the Effects of Magnetic Fields on the Arrangement of Surface Spins and the Catalytic Activity of Pd Nanoparticles, *ACS Appl. Mater. Interfaces*, 2015, **7**(11), 6019–6024.

31 W. Gao, J. Lu, S. Zhang, X. Zhang, Z. Wang, W. Qin, J. Wang, W. Zhou, H. Liu and Y. Sang, Suppressing Photoinduced Charge Recombination *via* the Lorentz Force in a Photocatalytic System, *Adv. Sci.*, 2019, **6**(18), 1901244.

32 L. Dloczik, O. Ileperuma, I. Lauermann, L. M. Peter, E. A. Ponomarev, G. Redmond, N. J. Shaw and I. Uhlendorf, Dynamic response of dye-sensitized nanocrystalline solar cells: characterization by intensity-modulated photocurrent spectroscopy, *J. Phys. Chem. B*, 1997, **101**(49), 10281–10289.

33 H. Okumura, S. Endo, S. Joonwichien, E. Yamasue and K. N. Ishihara, Magnetic field effect on heterogeneous photocatalysis, *Catal. Today*, 2015, **258**, 634–647.

34 R. Dhanalakshmi, P. R. Vanga, M. Ashok and N. V. Giridharan, The Effect of a 0.5 T Magnetic Field on the Photocatalytic Activity of Recyclable Nd-modified $BiFeO_3$ Magnetic Catalysts, *IEEE Magn. Lett.*, 2016, **7**, 2106904.

35 J. Li, Q. Pei, R. Wang, Y. Zhou, Z. Zhang, Q. Cao, D. Wang, W. Mi and Y. Du, Enhanced Photocatalytic Performance through Magnetic Field Boosting Carrier Transport, *ACS Nano*, 2018, **12**(4), 3351–3359.